Journal of Geophysical Research: Solid Earth

RESEARCH ARTICLE
10.1029/2018JB016816

Theory of Stable Multidomain Thermoviscous Remanence Based on Repeated Domain Wall Jumps

Thomas A. Berndt[1] **and Liao Chang**[1,2]

[1]Laboratory of Orogenic Belts and Crustal Evolution, School of Earth and Space Sciences, Peking University, Beijing, China, [2]Laboratory for Marine Geology, Qingdao National Laboratory for Marine Science and Technology, Qingdao, China

Key Points:
- Repeated domain wall jumps in multidomain particles yield an analytical expression for relaxation times and blocking temperatures
- MD grains have similar "Pullaiah" nomograms to SD grains, but with a different time-temperature relationship
- MD particles can be highly stable remanence carriers with respect to thermal demagnetization but can be very unstable under AF demagnetization

Correspondence to:
T. A. Berndt,
tberndt@pku.edu.cn

Citation:
Berndt, T. A., & Chang, L. (2018). Theory of stable multidomain thermoviscous remanence based on repeated domain wall jumps. *Journal of Geophysical Research: Solid Earth*, *123*. https://doi.org/10.1029/2018JB016816

Received 30 SEP 2018
Accepted 10 DEC 2018
Accepted article online 12 DEC 2018

Abstract We developed a theory of multidomain (MD) thermoviscous remanence that can be solved analytically to yield an expression relating the blocking temperature of a MD grain to its relaxation time. This expression is analogous to Néel's widely used theory of single-domain (SD) thermoviscous remanence but yields a different time-temperature relationship. The theory is based on a two-domain model with a domain wall (DW) that can jump between different pinning sites. In contrast to previous theories of this kind, our theory considers repeated DW jumps rather than a single jump in isolation. It is shown that while SD remanence behavior is fully described by the two quantities (V, H_{K0}), that is, volume and microscopic coercivity, MD particle remanence depends on three quantities: volume, Barkhausen volume, and DW pinning field, denoted (V, V_{Bark}, H_{K0}). "Pullaiah" nomograms of this new theory show that while small MD grains behave almost identically to SD grains, larger grains show different slopes depending on the above quantities. The theory predicts that MD grains can be highly stable remanence carriers, in particular showing a high thermal stability. Grains with weak pinning fields, however, while thermally stable, are highly unstable under alternating field (AF) demagnetization, being demagnetized under fields of a few millitesla. Our theory also explains (1) why samples dominated by MD grains show curved vector demagnetization plots for both thermal and AF demagnetization, as well as (2) why MD grains affect thermal demagnetization plots even at high temperatures, while their remanence is completely removed within the first few AF demagnetization steps.

1. Introduction

The field of paleomagnetism relies on one general principle: the fact that magnetic mineral grains in rocks can acquire a remanent magnetization as a result of an ambient magnetic field at high temperatures and preserve the remanence over geological timescales at low temperatures. A theory of this principle, termed thermoremanence (or thermoviscous remanence if large timescales are involved), was developed by Néel (1949) for magnetically uniform single-domain (SD) particles and has since been used for a variety of purposes, from plate tectonic reconstructions, over the study of climate variability (Kitaba et al., 2013), dating of tsunamis and floods (Berndt & Muxworthy, 2017; Muxworthy et al., 2015; Sato et al., 2014), the evolution of early life on Earth (Tarduno et al., 2014), to the formation of the solar system (Fu et al., 2014), and even hominid extinction (Valet & Valladas, 2010). The success of Néel's theory is probably due to (1) its wide-ranging implications, (2) its simplicity, and (3) the lack of adequate alternative theories for nonuniform magnetic particles (as explained below).

It is now known, however, that much of the remanence carried by natural samples is not due to SD grains, but to nonuniformly magnetized larger grains. These may range from flowering (almost SD) states, over vortex/pseudo–single domain (PSD) states (e.g., Almeida et al., 2016; Day, 1977; Shah et al., 2018), to true multidomain (MD) grains, that is, grains with several uniformly magnetized areas (domains) that are separated by domain walls (DW). Currently, no theory of nonuniformly magnetized grains is generally accepted and/or widely used. Instead, often SD theory is used despite its inapplicability (when exact blocking temperatures are not important) or numerical models are used to assess domain stability (mostly for vortex/PSD grains) or empirical models of MD grains are considered (mostly to model paleointensities). A few attempts at developing a physical theory of MD thermoremanence have been made, but none of them have found wide acceptance.

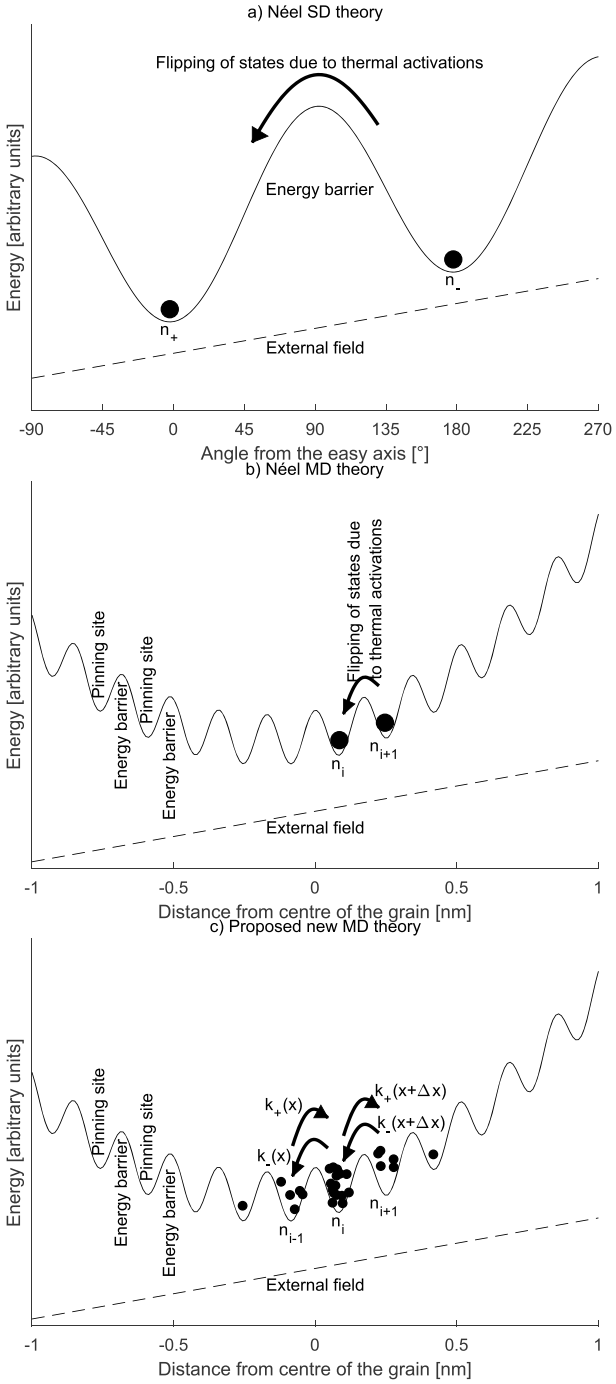

Figure 1. Schema of the different physically motivated theories: (a) Néel SD theory, (b) Néel MD theory, and (c) the new MD theory proposed here based on repeated domain wall jumps (for clarity, the schema shows a sinusoidal pinning field, but the derivations are done for a sawtooth pinning field). SD = single domain; MD = multidomain.

1.1. Physical Models of MD Thermoremanence

Néel's SD theory predicted a simple exponential relationship between the relaxation time τ and the blocking temperature T_B of a grain that is controlled by thermal energy that allows the magnetic moment vector of a grain to spontaneously jump the energy barrier separating its two stable states (Figure 1a):

$$\tau_{SD} = \tau_0 \exp\left\{\frac{\mu_0 V M_s H_K}{k_B T}\left(1 - \frac{|H|}{H_K}\right)^2\right\}, \text{ (in field)} \quad (1)$$

$$\tau_{SD} = \frac{\tau_0}{2} \exp\left\{\frac{\mu_0 V M_s H_K}{k_B T}\right\}, \text{ (zero field)} \quad (2)$$

where τ_0 is a constant called the attempt time, μ_0 is the vacuum permeability, V is the volume of the grain, M_s is the spontaneous magnetization, H_K is the microscopic coercivity (i.e., the difference in self-demagnetizing fields along the easy and hard axes), k_B is the Boltzmann constant, and H is the external applied field. The equilibrium magnetization M_{eq} of an ensemble of identical SD grains is given by a Maxwell-Boltzmann distribution of the two energy minima, yielding

$$M_{eq,SD} = M_s \tanh\left\{\frac{VHM_s(T)}{k_B T}\right\} \approx \frac{VHM_s^2(T)}{k_B T}. \quad (3)$$

Later, Néel (1955) extended his theory to MD grains (Figure 1b). This theory is based on the assumption that large magnetic particles will form DWs that separate different areas of uniform magnetization to form magnetic domains. It further assumes that natural minerals will generally have various local energy minima due to impurities, crystal lattice defects, cracks, nonmagnetic inclusions, etc. These energy minima, termed pinning sites (PS), are preferred locations for DWs: DWs are pinned to them. DWs therefore do not freely move and follow changes in the external magnetic field but remain pinned to the PS, unless the field is increased to certain threshold value, at which point, the DW "breaks off" the pinning and jumps to another nearby PS—a process called a Barkhausen jump. Néel (1955) not only derived the field necessary to induce such a jump (the coercivity of the pinning field), which is found to depend on the maximum gradient of the potential barrier (not on its height), but also derived expressions for the energy necessary to form DWs (i.e., forming multiple domains rather than remaining SD) and derived stable domain structures of MD grains. Based on this, Everitt (1962) and Schmidt (1973) calculated relationships between blocking temperatures and relaxation times for such isolated DW jumps: The relaxation time in this case is the time it takes a DW to jump from its current position to a neighboring position. During this process, the DW movement sweeps out a volume that is called the Barkhausen volume V_{Bark}. The resulting expression for the relaxation time is therefore formally almost identical to its SD equivalent, with the exception that it depends on the Barkhausen volume rather than the grain volume and H_K is due to the pinning field, rather than the demagnetizing field.

$$\tau_{MD} = \tau_0 \exp\left\{\frac{c\mu_0 V_{Bark} M_s H_K}{k_B T}\right\}, \quad (4)$$

where c is a constant that depends on the shape of the function used to model the pinning field: for example, 1 for a sawtooth function, and $2/\pi$ for a sinusoidal function. The equilibrium magnetization is simply given by

$$M_{eq,MD} = \frac{H}{N}, \quad (5)$$

where N is the demagnetizing factor of domain structure. N is an approximately linear function of $1/n$, where n is the number of domains, being 0.127 for a two-domain grain and approaching the value of a SD cube (1/3) for an infinite number of domains (Dunlop, 1983). Gaunt (1977) further showed that the preexponential frequency factor/the attempt time τ_0 is different for DW movement compared to coherent rotation of SD grains. Building on this theory, Dunlop and Xu (1994) and Xu and Dunlop (1994) developed theories of partial thermoremanent magnetization (pTRM) acquisition of MD grains with repeated identical and nonidentical energy barriers to DW motion, respectively. Many other works focused on high-field (i.e., hysteresis) properties rather than thermal effects (Bertotti et al., 1999; Church et al., 2011; Cizeau et al., 1997; Pike et al., 2001).

The important feature common to all these theories is that they are all based on the assumption that blocking depends on the occurrence of a single Barkhausen jump of a DW from its current PS to a neighboring PS. Therefore, the blocking condition is given by equation (4) in all these theories. As their basis is formed by the work of Néel (1955), we will refer to all such theories as Néel-type MD theories.

Shcherbakov et al. (1993), following McClelland-Brown and Sugiura (1987), proposed a theory accounting for temperature-dependent domain structures: It divides a grain into a number of cells, each of which can be magnetized in either a positive or a negative direction with respect to the applied field, in a similar fashion to SD grains. They then assume that each of the cells may switch its state on cooling and calculate how the

domain structure changes as a function of temperature. This is, as the authors point out, effectively similar to a set of strongly interacting SD grains. They propose that the main mechanism responsible for thermoremanent magnetization (TRM) acquisition is not DW jumps, but rather finding the lowest energy domain configuration as temperature decreases. By construction, this theory only allows for remanence acquisition under temperature changes (i.e., cooling), which may be reasonable for TRMs, but it does not treat the time dimension, that is, viscous, thermoviscous, and cooling rate-dependent effects. Building on the model by Shcherbakov et al. (1993), two subsequent works (Biggin and Poidras, 2006; Biggin, 2006) showed that thermal remanence acquisition and thermal demagnetization of MD grains are symmetrical to first order, which allowed them to show some implications of the theory for paleointensity, such as the failure to pass pTRM checks even in the absence of thermal alterations.

1.2. Empirical Models of MD Thermoremanence

Various models have been proposed that aim to reproduce some of the features of MD samples that are often observed experimentally, such as the difference in blocking and unblocking temperatures, pTRM tails, the field dependence of TRM, and the curvature in Arai plots in Thellier and Thellier (1959) type paleointensity experiments. Fabian, (2000, 2001) developed a purely phenomenological mathematical framework to describe ensembles of particles with any combination of blocking and unblocking temperatures. This allows to mathematically describe any observed TRM features without making any reference to the underlying physical principles causing the remanence. Fabian (2003) derived a statistical theory that assumes that MD grains may have various stable states that can switch between each other and can be described by a Markov process. This model allows to show certain properties of MD TRMs such as the linearity of TRM with the field, the additivity of pTRMs in weak fields, and the difference in blocking and unblocking temperatures. However, it does not aim to assign any physical meaning to the nature and magnitude of the energy barriers but rather describes them purely statistically. A similar model was also used to predict domain state stabilization by iterated thermal magnetization processes (Fabian & Shcherbakov, 2004). By construction, the various empirical models of MD thermoremanence are relatively successful at modeling the experimentally observed effects of MD samples but have relatively little predictive power of MD effects due to their limited physical basis.

1.3. Numerical Models of MD Thermoremanence

Micromagnetic models allow to numerically solve the physical equations that govern the magnetization of a magnetic mineral, allowing to obtain domain structures of particles of any shape given the magnetic material properties and the ambient magnetic field. Some magnetic properties, (e.g., spontaneous magnetization, demagnetizing fields, and anisotropy) depend on temperature, and so the stable domain states of some grains have been calculated as a function of temperature using micromagnetic models (Muxworthy & Williams, 1999). However, key to the thermal stability of remanent magnetizations is the blocking, that is, the energy barrier between the different local energy minima (Fabian et al., 1996). Once these energy barriers are found, they can be used to obtain relaxation times from the Arrhenius equation also used in Néel's SD and MD theories. This process has to be repeated for all temperatures in question and all grain sizes, geometries, and minerals of interest and has been done for magnetite cubes (Muxworthy et al., 2003) and more recently using the general micromagnetic model MERRILL (Conbhuí et al., 2018) for equidimensional magnetite cuboctahedra (Nagy et al., 2017), for greigite octahedra (Valdez-Grijalva et al., 2018), and for iron cubes (Shah et al., 2018). While such micromagnetic models are on the rise and are undoubtedly physically most accurate, they have a number of shortcomings: (1) the great computing power necessary to calculate large particles limits them mostly to the PSD range, that is, vortex states rather than true MD states that contain DWs; (2) as the model has to be run for a particular grain geometry, a nearly infinite number of calculations would have to be done to cover all naturally occurring grain sizes and shapes; (3) unlike simple models like Néel's SD and MD theories, they do not allow an intuitive understanding of the underlying reasons for the remanence, as the results are obtained purely numerically; and (4) they require a level of detail of sample characterization to be run that is well beyond all but the most advanced paleomagnetic studies and hence are of limited use for most studies.

1.4. Why Another Model of MD Remanence?

All of the currently existing approaches to explain MD remanence have their unique advantages and shortcomings, but none of them has generally been proven to be successful: Physical models fail to explain many of the experimentally observed effects, empirical models can fit experimental data but cannot explain them in terms of the underlying physics, and numerical models are too impractical and restricted to PSD sizes. Also, some of the physical models are built to explain thermoremanence only but cannot explain viscous or

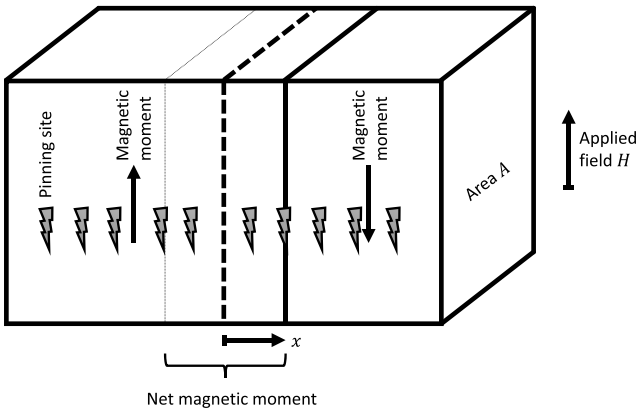

Figure 2. Schema of a one-DW (bold line) multidomain grain with repeated identical pinning sites (flashes). The DW is displaced from its equilibrium position (dotted line) by a distance x. DW = domain wall.

thermoviscous remanence. Hence, a model that is similar to SD theory in terms of simplicity, yet is based on accurate physical principle, should be built. In this paper we develop a theory that, starting from Néel's MD theory, goes one step further toward this goal. The theory described here is for true MD grains rather than vortex/PSD grains, that is, grains that are large enough to contain at least one DW and is aimed to predict thermoviscous remanence, that is, remanence acquisition well below the Curie temperature. This is important in order to assess the stability of MD remanence, as models of pure thermoremanence can only predict what remanence MD grains acquire at high temperatures, but not over what timescales they can preserve this remanence.

2. Theory

We start from Néel's MD theory, where a grain is considered to be divided into areas of uniform magnetization, separated by a DW of surface area A at position x (Figure 2), where we assume for simplicity that the origin is at the center of the grain. The energy of the system is given by the sum of the *magnetostatic energy*, that is, the energy due to the net magnetic moment M of the grain in an external applied field H; the *(self-)demagnetizing energy*, that is, due to the net magnetic moment M of the grain inside the field created by itself (which is itself proportional to M); and the DW *pinning energy*, which is due to crystal imperfections, inclusions, etc. This can be written

$$E(x) = -2\mu_0 A M_s H x + \frac{2\mu_0 N M_s^2 A^2 x^2}{V} - \mu_0 H_K M_s V_{\text{Bark}} P\left(\frac{x}{\Delta x}\right), \tag{6}$$

where A is the surface area of the DW and N is the demagnetizing factor due to the domain structure (0.127 in the two-domain case; Dunlop & Özdemir, 1997). The wall pinning energy can be modeled by any cyclic function $P(x/\Delta x)$, for example, a sinusoid (Figure 1c), but here we assume for simplicity a sawtooth function that is 0 at integer values (i.e., if x is a multiple of Δx, the PS) and 1 at half integer values (i.e., between the PS). Therefore, Δx is the distance between two neighboring wall PSs. As DWs can only jump from one PS to the next, the volume swept out by the DW during a jump is $V_{\text{Bark}} = A\Delta x$, the Barkhausen volume. While the first two terms in equation (6) are physically derived (Néel, 1955), the third term is chosen to model a periodic pinning field—the coefficients in front of this function are therefore somewhat arbitrary. Following the reasoning of Schmidt (1973), it should have a temperature dependence following a power law of the spontaneous magnetization, since so do the two most likely contributors to the interaction between DWs and PS: magnetostriction and magnetic anisotropy. Schmidt (1973) investigated powers between 2 (more representative for the former) and 10 (more representative for the latter); for simplicity, here we will continue the treatise using a square dependence, just like the self-demagnetizing energy term. Note that the coefficient H_K here has no a priori physical meaning (unlike all the other coefficients in the pinning field term): Therefore, redefining H_K, the equation could be written with only the H_K coefficient, in which case H_K would be in units of energy and would describe the magnitude of the (unknown) pinning field. Here, however, we chose to define H_K in such a way that the pinning field is given by the product of the various coefficients in the third term. If we further define $H_K(T) = H_{K0}M_s(T)/M_{s0}$, this assures the quadratic temperature dependence proposed by Schmidt (1973). Furthermore, the notation is chosen such that applying an external field $H = H_K$ will cause an immediate *field-induced* DW jump from the equilibrium position (where the self-demagnetizing term is 0): If $H = H_K$, then the magnetostatic term at $x = \Delta x/2$ (the position of the DW energy barrier) equals the pinning term—hence, the energy barrier is overcome (H_K, the field such that the slope of the energy function is 0; Néel, 1955; note that the derivative of P is always ± 1). There is hence an analogy between the H_K here and the microscopic coercivity of an SD grain $H_{K,\text{SD}}$: Even though physically the two are unrelated both of them refer to the field that one would have to apply *in the absence of thermal fluctuations* to induce a change of remanent state. Therefore, we can consider H_K the *coercivity of pinning*. The Néel (1955) type MD theories are mainly concerned with such field-induced DW jumps and their temperature dependence.

Next, we note that the net magnetization of the grain is given by

$$M = \frac{2M_s Ax}{V}, \tag{7}$$

where the factor 2 comes from the fact that the net magnetic moment is due to twice the volume swept out by the DW displacement from the center of the grain (Figure 2). The energy can therefore be written more compactly

$$E(x) = \mu_0 V\left(\frac{1}{2}NM^2 - HM\right) - \mu_0 H_K M_s V_{\text{Bark}} P\left(\frac{x}{\Delta x}\right). \tag{8}$$

From here, we will start to deviate from Néel-type MD theories. We note that each PS at position x has two energy barriers, one to the left, ΔE_-, and one to the right, ΔE_+. The energy barrier between two neighboring wall PSs is given by

$$\Delta E_\pm = E\left(x \pm \frac{1}{2}\Delta x\right) - E(x). \tag{9}$$

While Néel-type MD theories are concerned with calculating (field-induced) jumps over only one barrier, here we will consider the effect of repeated jumps over many such barriers—as jumps can occur in either direction. For a large assembly of identical MD grains, each grain may potentially have its DW in any of the available PS locations x, following some statistical distribution $p(x)$. Each of these DWs may jump (1) both left and right and (2) after each jump the DW may jump again (left or right) from its new location, leading to a continually evolving distribution of DW locations. In order to predict the behavior of the ensemble, we start the treatise by first calculating the magnitude of all the energy barriers and then calculating the frequencies of jumps occurring over any of them. Assuming Δx is small, the energy barriers are given by the derivative of $E(x)$, multiplied by Δx, which is (neglecting higher-order terms of Δx)

$$\Delta E_\pm \equiv \mu_0 V_{\text{Bark}} M_s \left(\pm(NM - H) + H_K\right). \tag{10}$$

Analogous to the reasoning of Néel-type theories, the rate coefficients for a DW jumping over a barrier (Barkhausen jump) are given by an Arrhenius equation

$$k = \frac{1}{\tau_0}\exp\left\{-\frac{\Delta E}{k_B T}\right\}. \tag{11}$$

For each PS (at position x), we have therefore two rate coefficients, k_- is the rate at which jumps occur to the left, and k_+ is the rate it which jumps occur to the right:

$$k_\pm = \frac{1}{\tau_0}\exp\left\{-\frac{\mu_0 V_{\text{Bark}} M_s\left(\pm(NM - H) + H_K\right)}{k_B T}\right\}. \tag{12}$$

Now again, we deviate from Néel-type theories by noting that real samples do not only consist of a single MD grain but contain a large number of grains: Each of these grains can in general be found in any of the states x (Figure 1c). That is, the DW of an ensemble of identical MD grains will not all be in the same state, even if they have experienced the same thermomagnetic history—instead the DW positions will follow a statistical distribution (it can be shown that equation (11) leads to a Maxwell-Boltzmann distribution). The total magnetization of the grain is then given by the integral over all these grains. If the probability of finding a DW of a given grain at PS x is given by $p(x)$, then this can be expressed as the integral of the magnetization over all the possible states times their probability, that is,

$$M_{\text{tot}} = \int p(x)M(x)\,\mathrm{d}x. \tag{13}$$

As we want to derive an expression for the stability of the magnetization over time (i.e., the relaxation time), we first derive the rate of change of the probability distribution. For any PS at location x, this rate of change is given by the rates DWs jump into the state x from left ($k_+(x - \Delta x)$) and from right ($k_-(x + \Delta x)$), minus the rates at which DWs jump out of state x, toward the left (k_-) and toward the right (k_+), each of them multiplied by the probability of finding DWs at the respective locations:

$$\frac{\mathrm{d}p}{\mathrm{d}t} = -p(x)\left[k_+(x) + k_-(x)\right] + p(x-\Delta x)\,k_+(x-\Delta x) + p(x+\Delta x)\,k_-(x+\Delta x). \tag{14}$$

The probabilities and frequencies at the neighboring locations ($x \pm \Delta x$) can be approximated by the first two terms of their respective Taylor expansions

$$p(x \pm \Delta x) \approx p(x) \pm \frac{\mathrm{d}p}{\mathrm{d}x}\Delta x, \tag{15}$$

$$k_\pm(x \pm \Delta x) \approx k_\pm(x) \pm \frac{\mathrm{d}k_\pm}{\mathrm{d}x}\Delta x. \tag{16}$$

Hence, ignoring higher-order terms,

$$\frac{\mathrm{d}p}{\mathrm{d}t} = -p\frac{\mathrm{d}\left(k_+ - k_-\right)}{\mathrm{d}x}\Delta x - \frac{\mathrm{d}p}{\mathrm{d}x}\left(k_+ - k_-\right)\Delta x. \tag{17}$$

The derivatives of $k_\pm$ are easily found to be

$$\frac{\mathrm{d}k_\pm}{\mathrm{d}x} = \mp\frac{2\mu_0 N M_s^2 A V_{\mathrm{Bark}}}{k_B T V}k_\pm. \tag{18}$$

Hence, equation (17) can be expressed as

$$p = \frac{k_B T V}{2\mu_0 N M_s^2 V_{\mathrm{Bark}}}\left(\frac{1}{A}\frac{\mathrm{d}p}{\mathrm{d}x}\left(\frac{k_+ - k_-}{k_+ + k_-}\right) + \frac{1}{V_{\mathrm{Bark}}}\frac{\mathrm{d}p}{\mathrm{d}t}\left(\frac{1}{k_+ + k_-}\right)\right), \tag{19}$$

We now note that the rate coefficients k_+ and k_- are exponential functions with opposite signs, such that their terms in equation (19) can be expressed as hyperbolic functions

$$\frac{k_+ - k_-}{k_+ + k_-} = \tanh\left\{-\frac{\mu_0 V_{\mathrm{Bark}} M_s (NM - H)}{k_B T}\right\} \approx -\frac{\mu_0 V_{\mathrm{Bark}} M_s (NM - H)}{k_B T}, \tag{20}$$

where the approximation holds if V_{Bark} is small, the applied field is small, and the magnetization is not too far from equilibrium. Similarly,

$$\frac{1}{k_+ + k_-} = \frac{\tau_0}{2}\exp\left\{\frac{\mu_0 V_{\mathrm{Bark}} M_s H_K}{k_B T}\right\}\mathrm{sech}\left\{-\frac{\mu_0 V_{\mathrm{Bark}} M_s (NM - H)}{k_B T}\right\}, \tag{21}$$

which is, making the same approximation,

$$\frac{1}{k_+ + k_-} \approx \frac{\tau_0}{2}\exp\left\{\frac{\mu_0 V_{\mathrm{Bark}} M_s H_K}{k_B T}\right\}. \tag{22}$$

Therefore, we now obtain the following partial differential equation for the probability distribution

$$p = -\frac{V(NM - H)}{2NM_s A}\frac{\mathrm{d}p}{\mathrm{d}x} + \frac{1}{\tau}\frac{\mathrm{d}p}{\mathrm{d}t}, \tag{23}$$

where in anticipation of the relaxation time τ we defined

$$\tau = \frac{\tau_0 k_B T V}{4\mu_0 N M_s^2 V_{\mathrm{Bark}}^2}\exp\left\{\frac{\mu_0 V_{\mathrm{Bark}} M_s H_K}{k_B T}\right\}. \tag{24}$$

Now we are able to obtain the change of the total magnetization over time by integrating this equation with respect to x, that is, over all possible states. Noting that the integral of p over x is unity (since p is a probability distribution), using partial integration, and making the assumption that the probability of finding a DW at any of the boundaries of grains is 0 (which is a good approximation for small external fields and temperatures well below the Curie point), and finally using equation (13) to replace the integrals by M_{tot}, one eventually obtains

$$M_{\text{tot}} = M_{eq} - \frac{\tau_0}{\tau}\frac{\mathrm{d}M_{\text{tot}}}{\mathrm{d}t}, \tag{25}$$

where

$$M_{\text{eq}} = \frac{H}{N}. \tag{26}$$

This equation is formally equivalent to the well-known equation from SD theory, so we know that the solution must be

$$M = (M_0 - M_{\text{eq}})e^{-t/\tau} + M_{\text{eq}}, \tag{27}$$

where M_0 is the initial magnetization at time 0. The magnetization of an ensemble of identical MD grains changes exponentially with time just like an ensemble of identical SD grains; note that the relaxation time τ is given by equation (24), which has additional preexponential factors compared to Néel's SD and MD theories.

3. Results

For convenience, let us reiterate the blocking relations for Néel SD, Néel MD, and our MD theory here:

$$\tau = \tau_0 \exp\left\{\frac{\mu_0 V M_s H_K}{k_B T}\left(1 - \frac{|H|}{H_K}\right)^2\right\}, \text{ (SD, in field)} \tag{1 revisited}$$

$$\tau = \frac{\tau_0}{2}\exp\left\{\frac{\mu_0 V M_s H_K}{k_B T}\right\}, \text{ (SD, zero field)} \tag{2 revisited}$$

$$\tau = \tau_0 \exp\left\{\frac{c\mu_0 V_{\text{Bark}} M_s H_K}{k_B T}\right\}, \text{ (Néel MD)} \tag{4 revisited}$$

$$\tau = \frac{\tau_0 k_B T V}{4\mu_0 N M_s^2 V_{\text{Bark}}^2}\exp\left\{\frac{\mu_0 V_{\text{Bark}} M_s H_K}{k_B T}\right\}, \text{ (our MD)} \tag{14 revisited}$$

And the equilibrium magnetizations are given by

$$M_{\text{eq}} = \tanh\left\{\frac{VHM_s(T)}{k_B T}\right\} \approx \frac{VHM_s(T)}{k_B T}, \text{ (SD)} \tag{3 revisited}$$

$$M_{\text{eq}} = \frac{H}{N}, \text{ (Néel and our MD)} \tag{5 revisited}$$

3.1. Comparing Néel-Type SD and MD Theories

Comparing the Néel SD and MD equations (note that for small fields, the only difference between equations (1) and (2) is the factor 2 in front of the exponential), we see that both of them are exactly the same, except for (1) the factor c, (2) the replacement of V by V_{Bark}, and (3) the different meaning of H_K (coercivity of coherent rotation vs. coercivity of pinning). Regarding (1), c is a factor close to 1 that depends on the shape of the pinning field and would be exactly unity for the sawtooth potential used here. Regarding (3), the different meaning of H_K is for most practical purposes largely irrelevant, since one rarely calculates the coercivity from first physical principles but rather infers it from measurements of the effective coercivity H_c, that is, from hysteresis loops or similar. Therefore, the only real difference in Néel-type SD and MD theories is the fact that in the former, the relaxation time depends on the grain volume, whereas in the latter it depends on the Barkhausen volume. This conclusion is hardly surprising, given that Néel-type MD theories are derived for isolated single Barkhausen jumps: The system is essentially a two-state system where the DW can only jump back and forth between the same two PS. This is equivalent to the SD model, where the magnetic moment can jump back and forth between the two states given by the anisotropy of the grain. While Néel-type MD theories are useful to predict field-induced jumps (i.e., a single jump over a number of barriers in the presence of a large field), we can conclude that in terms of thermal fluctuations they do not capture the essence of MD: the fact the DWs can be in many different PS.

3.2. Comparing Néel-Type and Our MD Theory

Next, let us compare our new MD theory to Néel-type MD theories. Equations (4) and (24) show that the exponential dependence is the same in the two (c is unity for a sawtooth pinning field). However, our theory predicts a *further linear dependence* of the relaxation time on

$$\frac{k_B T V}{4\mu_0 N M_s^2 V_{\text{Bark}}^2}. \tag{28}$$

Note that this factor is independent of H_K, which means that it is independent of the way the pinning field is modeled. In fact, the factor is due to the repeated nature of DW jumps that can occur in either direction. Since $M_s(T)$ is a decreasing function of temperature, this factor (1) increases τ with increasing temperature and increasing grain volumes, and (2) decreases with increasing Barkhausen volumes. Since the exponential is a decreasing function of temperature and an increasing function of the Barkhausen volume, the net effect of this new factor is that it (1) reduces the temperature dependence, (2) reduces the V_{Bark} dependence and (3) introduces a (positive) grain volume dependence. Moreover, this deviation from Néel SD and MD theory is most pronounced for small pinning coercivities H_K, in which case the exponential is less dominant in the equation; for large H_K however, the relaxation time versus temperature function will follow the same trend as SD grains (i.e., there would be some SD grain with H_K and V such that its relaxation time is equal to this MD grain at all temperatures). We can therefore divide MD grains into two categories: *strongly pinned* and *weakly pinned* MD grains. Strongly pinned MD grains largely follow Néel SD/MD theory: Because their energy barriers are large, they are rarely overcome by thermal fluctuations, and if they are, they will rarely be overcome again; that is, the single-DW jump/two-state model is a good approximation. We can conclude that given sufficiently strong pinning, an MD grain would have a similar thermoviscous stability to SD grains. For the remainder of the discussion we will therefore focus on weakly pinned MD grains.

The intuitive explanation of the different temperature dependence for weakly pinned MD grains is the following: If pinning is weak, energy barriers will be overcome rather frequently. However, this does not reset the grain's remanent magnetization: It rather changes its remanence by only one Barkhausen volume. If the Barkhausen volume is small (i.e., there are many PS), the change in magnetization due to a single jump is therefore negligible. Following the jump, there is a certain probability that the DW will jump back to where it came from. Only after a large number of jumps occurred into one direction (and only a small number of jumps back), will the magnetization change significantly. Roughly speaking, if n jumps are necessary to reach a new equilibrium position, then the time it takes to reach it will be n times the relaxation time of a single Barkhausen jump.

The effect of repeated PS is also apparent in the equilibrium magnetization: Our MD theory, just like Néel-type MD theories, predicts an equilibrium magnetization that is linear in H (equation (5)). This is due to the fact that a DW can "follow" the applied field to any PS location inside the grain corresponding to equilibrium—this is unlike SD grains, where the equilibrium magnetization is due to the difference in the numbers of grains in the state aligned with the field and opposing the field, respectively. The equilibrium magnetization derived in our theory is the same as that from Néel-type MD theories, but the explanations are different: In Néel-type MD theories, all the grains are expected to be found with their DWs in the equilibrium positions, whereas in our theory, only the statistical average of the DW locations centers around the equilibrium position.

3.3. Predictions for the Thermoviscous Stability of MD Grains

We are now in the position of making some predictions for ensembles of MD grains. First of all we note that while SD grains of a given mineral are fully described by the two parameters (V, H_K) (or (V, N) if one assumes shape anisotropy), MD grains in our theory are fully described by the three parameters $(V, V_{\text{Bark}}, H_K)$ We can use these three parameters to plot Pullaiah et al. (1975) nomograms (Figure 3). Nomograms are contour plots where at any given temperature and time all lines to the left indicate unblocked grains (i.e., those in their equilibrium state) and all lines to the right indicate blocked grains (i.e., those in their remanent state). There are two ways to read them: First, to assess the stability of a TRM, one finds the line at the temperature and time of remanence acquisition (e.g., 1 min for fast cooled lavas, at say 300 °C) and follows it to room temperature to read off the timescale over which the remanence is stable. Second, to assess the stability of a viscous remanent magnetization (VRM), one finds the line at room temperature for the time of VRM acquisition and follows it to laboratory timescale (e.g., 1 min) to read off the temperature that is necessary to remove the VRM in a thermal demagnetization experiment. Figure 3 shows six such nomograms (given that there are three

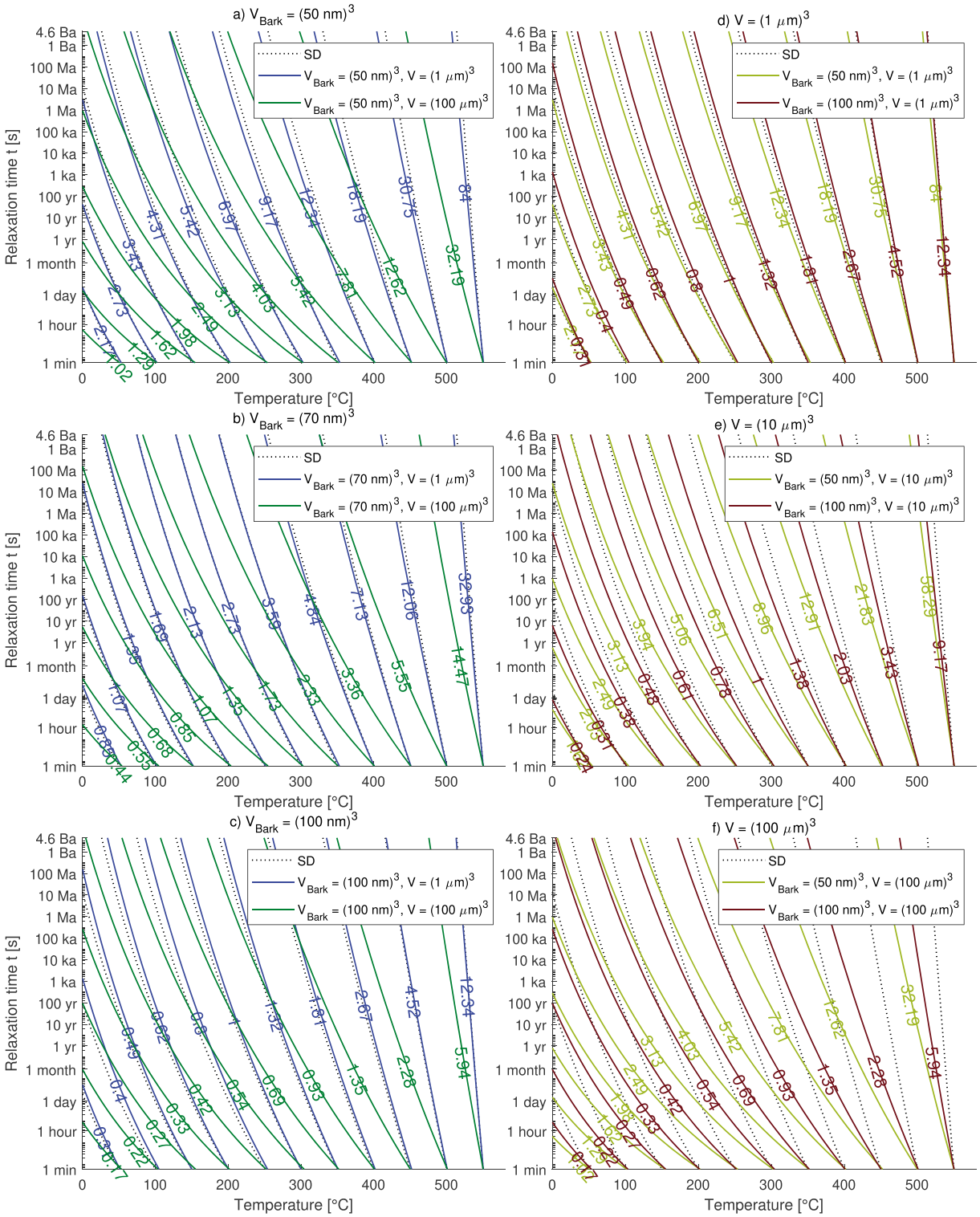

Figure 3. Nomograms. Black dotted lines indicate Néel SD theory, colored lines indicate our new multidomain theory. (a–c) Plots for three fixed Barkhausen volumes and (d–f) plots for three fixed grain volumes. Numbers on the nomograms indicate H_K in millitesla. SD = single domain.

parameters necessary to describe a MD grain, it is difficult to visualize them all in one plot). All of them show traditional Pullaiah nomograms based on Néel SD theory with dotted black lines for comparison, but note that nomograms based on Néel-type MD theory would look exactly the same to the SD lines.

Figures 3a–3c show nomograms for MD grains with the fixed Barkhausen volumes of 50, 70, and 100 nm, respectively. Each of them shows two sets of nomograms, one for small grains with volume of $(1\ \mu m)^3$ (blue) and one for large grains with volume of $(100\ \mu m)^3$ (green). Similarly, Figures 3d–3f show nomograms for MD grains with the fixed grain sizes of 1, 10, and 100 μm, respectively. Each of them shows two sets of nomograms, one for small Barkhausen volumes of 50 nm^3 (yellow) and one for large Barkhausen volumes of 100 nm^3(red).

In Figure 3d, for small MD grains, it is seen that all these are almost identical to the SD nomograms. However, the H_K given on these nomograms differ between each other for the different Barkhausen volumes and generally differ from the SD coercivity $H_{K,SD}$. We can therefore conclude that small MD grains have a similar thermoviscous behavior to SD grains and that this is almost independent of the Barkhausen volume.

Investigating the large MD grains (100 μm) in Figure 3f, one finds that all of them have a much shallower slope than the SD contours. This is the effect of repeated DW jumps: In large grains many PS are available such that DW have to jump repeatedly in order to reach a new equilibrium state. This has implications for the thermoviscous stability of MD remanence: Let us consider an ensemble of large MD grains with 50-nm Barkhausen jumps (Figures 3a and 3f) and compare it to an SD ensemble. In natural samples both of the ensembles would be expected to have a large range of coercivities (pinning coercivity and coherent rotation coercivity, respectively), each of them corresponding to one line in the nomogram. Let us suppose that both samples got reheated to 150 °C and acquired a secondary pTRM. The SD sample would retain this secondary remanence for ∼10 Ma. For many paleomagnetic applications this would be considered a stable remanence. The MD ensemble on the other hand would retain the remanence only for 1 year, that is, it would not be a stable remanence. A similar conclusion is made when considering an ensemble of large MD grains with 100-nm Barkhausen volumes (Figures 3c and 3f): These grains would retain the remanence for 100 years, that is, would be unstable TRM carriers, although less so than the smaller Barkhausen volume ensemble.

This, however, does not mean that large MD grains are generally unstable remanence carriers. If the sample was heated to 300°, for example, then the large MD grains (Figure 3f) would be stable over timescales larger than the age of the Earth. Similarly, if the remanence is primary, that is, resulted from cooling through the Curie temperature, it would be stable. It should be noted though that our MD model made approximations that do not hold close to the Curie temperature (more about this in section 4), such that it cannot predict the remanence resulting from this. It does, however, predict that once the sample is cooled, this remanence should be stable over geological timescales. The conclusion that all MD grains can in principle carry stable thermoremanences is explained by the pinning coercivity: Given sufficiently large pinning coercivity, the energy barriers cannot be overcome at low temperatures (at sufficiently high temperatures, however, the energy barriers vanish, such that any grain can acquire a TRM). This is consistent with our previous reasoning that strongly pinned MD grains are stable remanence carriers.

In summary, we have found that (1) small MD grains behave like SD grains, (2) large MD grains are stable remanence carriers, but less so than SD grains, and (3) for large MD grains, those with large Barkhausen volumes (i.e., fewer PS) are more stable than those with small Barkhausen volumes.

Conversely, it is illustrative to consider samples that carry a viscous overprint that one aims to remove by thermal demagnetization. Again, small MD grains behave like SD grains (Figure 3d) such that a VRM acquired over ∼100 years needs to be heated to ∼ 100° to be removed, just like an SD sample. Large MD grains (Figure 3f), however, would have to be heated to ∼ 150° and ∼ 200° for 100 and 50-nm Barkhausen volumes, respectively. The conclusion is that large MD grains are more viscous than SD grains and need to be heated to higher temperatures to be cleaned thermally.

Further conclusions can be drawn about the coercivities of MD grains. Those grains with (1) small Barkhausen volumes and/or (2) small grain volumes need higher coercivities to have the same thermal stability as those with large Barkhausen volumes and/or grain volumes and low pinning coercivities (Figures 3d–3f). This is even true for small MD grains that otherwise behave like SD grains. This is analogous to SD grains, where those with a large grain size and small coercivity have the same thermal stability as those with a small grain size and high coercivity—the only difference is that for MD grains this dependence is on both grain volume and on Barkhausen volume.

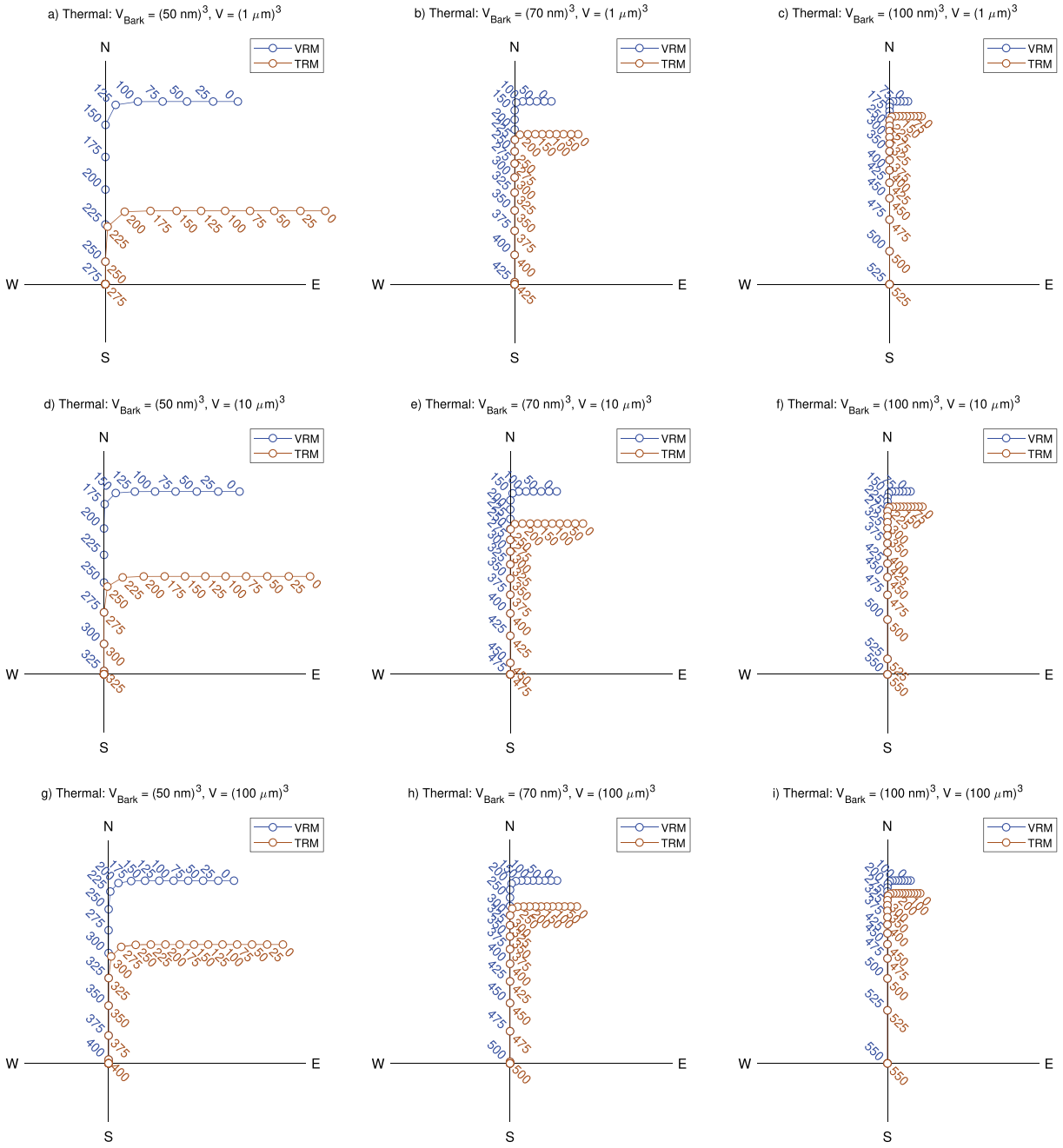

Figure 4. (a-i)Zijderveld plots of simulated stepwise thermal demagnetization of the multidomain ensembles shown in Figure 3. The blue plots simulate a primary TRM and a secondary VRM (680 ka); the brown plots simulate a primary TRM and a secondary partial TRM (100 °C, 100 ka). Labels show temperatures in degrees. TRM = thermoremanent magnetization; VRM = viscous remanent magnetization.

3.4. Predictions for Vector Demagnetization Plots

One of the most common procedures in paleomagnetism is the stepwise demagnetization of samples in order to remove any viscous or thermal secondary overprints and isolate the characteristic remanence (ChRM). This is most commonly done using either thermal or alternating field (AF) demagnetization and plotting the remaining remanence on Zijderveld (1967) plots. Here we present a number of simulated Zijderveld plots for MD samples containing a primary thermoremanence and one secondary overprint in a perpendicular direction. Simulations were done using the simple forward model from Berndt et al. (2017), adapted to account for MD relaxation times according to equation (24), for stoichiometric magnetite. The simulations were run (1) for secondary VRM acquired at room temperature over 680 ka (e.g., the Brunhes chron), and (2) for a secondary

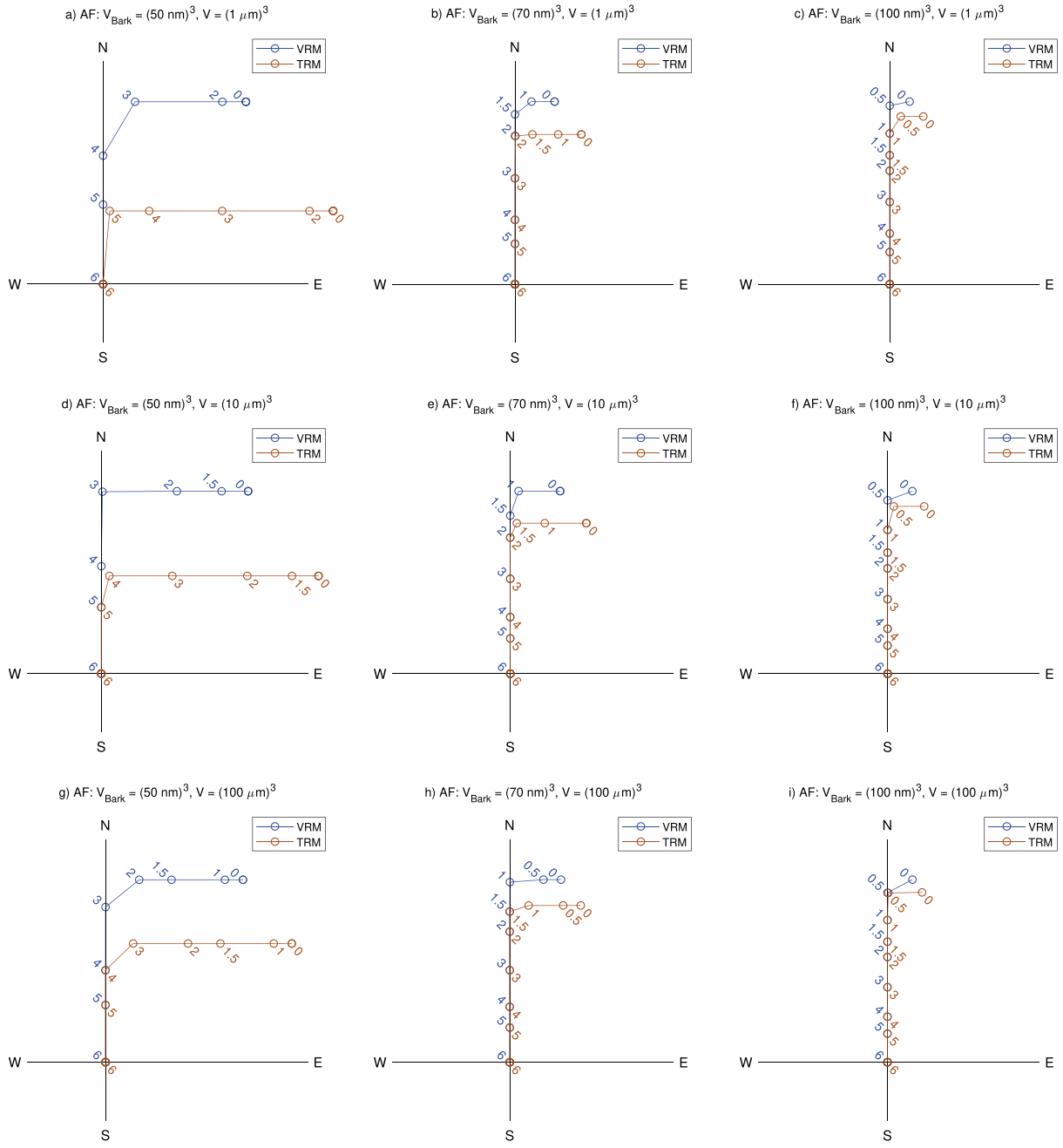

Figure 5. (a-i) Zijderveld plots of simulated AF demagnetization of the multidomain ensembles shown in Figure 3. The blue plots simulate a primary TRM and a secondary VRM (680 ka); the brown plots simulate a primary TRM and a secondary partial TRM (100 °C, 100 ka). Labels show AF peak fields in millitesla. AF = alternating field; TRM = thermoremanent magnetization; VRM = viscous remanent magnetization.

TRM acquired over 100 ka at 100 °C. All simulations assumed a frequency distribution of grains inversely proportional to the product of grain volume, Barkhausen volume, and pinning coercivity in order to approximate lognormal grain distributions that are common in natural samples.

Figure 4 shows the thermal demagnetization plots of the simulations, where each plot shows an ensemble with fixed grain volume and Barkhausen volume, that is, the ensemble contained grains only with varying pinning coercivity. In all of them, both the primary and the secondary remanence can be isolated easily. The plots show different intensities in the two components (i.e., lengths) due to the different strength of remanence depending on grain and Barkhausen volumes. Additionally, they show different unblocking temperatures of the overprint depending on grain volume, as was predicted in the nomograms (Figures 3a–3c). Some of

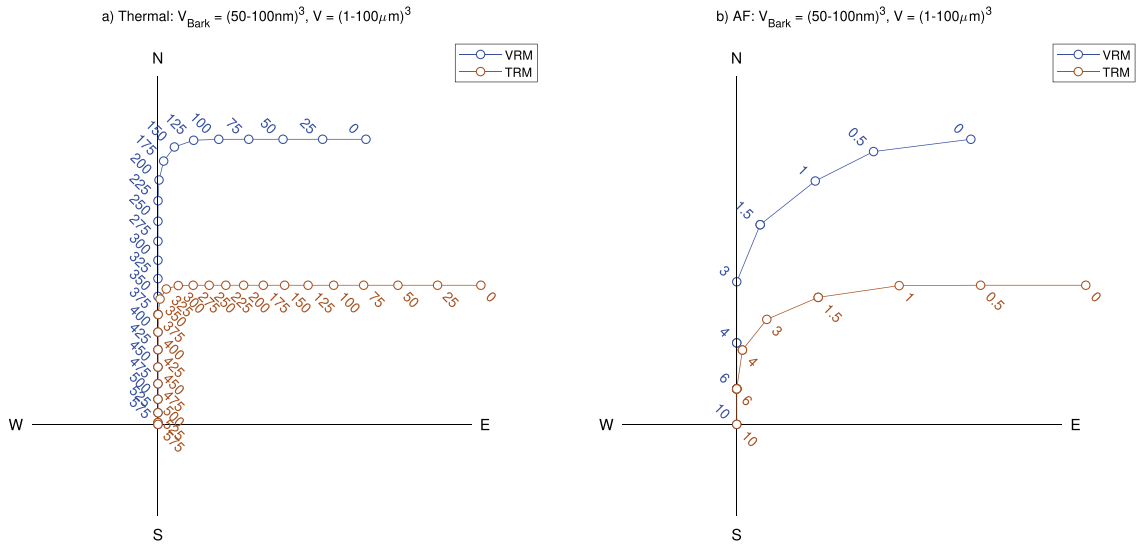

Figure 6. (a, b) Zijderveld plots of simulated AF demagnetization of the multidomain ensembles shown in Figure 3. The blue plots simulate a primary TRM and a secondary VRM (680 ka); the brown plots simulate a primary TRM and a secondary partial TRM (100 °C, 100 ka). Labels show AF peak fields in millitesla.
AF = alternating field; TRM = thermoremanent magnetization; VRM = viscous remanent magnetization.

the plots (Figure 4) show some level of curvature which is due to viscous relaxation on the timescale of the demagnetization experiment.

Figure 5 shows the same model for AF demagnetization. Both remanence components can be isolated for 50- and 70-nm Barkhausen volumes, but for 100-nm Barkhausen jumps, the secondary remanence is lost already after the first demagnetization step at 1 mT. For the smaller Barkhausen volumes the overprint is completely cleaned at slightly higher peak AF fields, with 4 mT being the maximum. The primary remanence in all the plots is removed around 6 mT. The low peak AF fields necessary to demagnetize MD samples is due to the low pinning coercivities (Figure 3), and is consistent with what has often been observed experimentally. Naturally, if one would chose an ensemble of grains with a large number of strongly pinned MD grains, these would result in higher AF fields—however, such ensembles would be impossible to acquire a viscous or thermal overprint (Figure 3).

In order to model a more realistic sample, Figure 6 shows thermal and AF demagnetization plots for an ensemble containing all grain volumes between 1 and 100 μm and all Barkhausen volumes between 50 and 100 nm. Again both plots show clear evidence of two magnetic components, and both plots permit isolation of the ChRM. In AF demagnetization, the VRM cannot be completely isolated, however, because it completely overlaps with the ChRM. All the plots show some curvature: for the VRM at 125–200 °C and 0–3 mT and for the pTRM at 300–350 °C and 0–8 mT. This is due to the fact that different MD grains have different thermal stabilities and different pinning coercivities for the same acquisition time and temperature (Figure 3). In Figures 4 and 5 this was visible in the different inflection points for each of the V and V_{Bark}; in Figure 6, the ensemble contains the grains of all these Zijderveld plots; hence, the curvature results from the superposition of all these inflection points. In summary, one can conclude, however, that even weakly pinned MD grains permit isolation of two remanence components fairly well, even though for AF demagnetization magnetic cleaning occurs at very low peak AF fields.

4. Discussion

The conclusions of our theory of repeated DW jumps of MD grains can be summarized as a flow chart (Figure 7): (1) strongly pinned MD grains behave just like SD grains because repeated DW jumps are rare due to high energy barriers; (2) small, weakly pinned MD grains behave similar to SD grains, because repeated DW jumps are rare due to the limited number of PS but have low coercivities (by definition); (3) large, weakly pinned MD grains are more viscous (i.e., TRMs are lost faster, or conversely, VRMs need higher temperatures

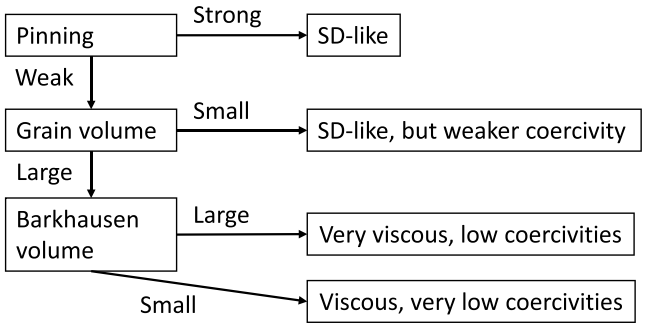

Figure 7. Categorization of the properties of multidomain grains.

to be removed) and have even lower coercivities. For these grains, larger Barkhausen volumes lead to higher viscosity, while smaller Barkhausen volumes lead to even lower coercivities.

4.1. Pinning Coercivities

Hence, a lot of the properties of MD grains depend on their pinning coercivities, which are not as easily determined as in the case of SD grains (e.g., for shape anisotropy the coercivity of coherent rotation is simply given by $H_{K,SD} = NM_s$). Néel (1944) gives the expression

$$H_K = \frac{5}{4}\sqrt{\frac{\pi^3}{8}}\frac{\gamma_W}{\mu_0 M_s r} \tag{29}$$

for the pinning coercivity that results from a nonmagnetic inclusion in the MD grain, where r is the radius of the inclusion and γ_W is the energy of a DW per unit area, which is given by $\gamma_W = 2\pi\sqrt{AK}$, which, for magnetite is around $\gamma_W = 0.93 \cdot 10^{-3}\,\mathrm{J/m^2}$. The expression is, however, meant for large (micrometer size) inclusions—for an inclusion of, say, 50 nm, H_K would be an unrealistic ~100 mT.

Independently of this, the theory described here makes no assumptions on the physical mechanism leading to DW pinning (other than temperature dependence proportional to the temperature dependence of $M_s^2(T)$, as argued by ; Schmidt, 1973). Hence, even though we do not currently have a theory to predict the pinning field in terms of the grain/crystal properties, we have here a theory where we can use H_K as just another magnetic parameter that can be determined from hysteresis experiments. We have found that if this parameter is very large ($\gtrsim$10 mT), the grain will be have like an SD grain. On the other hand, if H_K is very small, ($\lesssim$0.1 mT), the theory may predict a non-SD but yet stable thermoviscous behavior. However, for such weak pinning field-induced jumps become important compared to thermally induced jumps: A grain with $H_K \sim 50\mu$T, for example, immediately approaches equilibrium in the geomagnetic field because the energy barriers are overcome by the external field. Such a grain, even though stable in zero field, can practically be considered unstable because any remanence would be unlikely to survive the sample's transport to the laboratory. In the nomograms, those MD grains with large Barkhausen volumes, in particular those with large grain volumes had the lowest pinning coercivities (Figure 3c). This, however, does not mean that grains with large V, large V_{Bark} generally have low H_K—those with larger H_K are simply very stable from a thermoviscous point of view and only unblock close to their Curie temperatures (similar to SD grains): These correspond to the contour lines on the very right end of the nomograms (Figure 3).

4.2. Implications for Vector Demagnetization Plots

As shown in Figures 4–6, MD grains can be very reliable remanence recorders. Two major differences to SD grains exist, however: First, there is no one-to-one relationship between the unblocking temperature and the acquisition temperature/time. In pure SD samples, all the grains that have experienced the same thermomagnetic history will have the same blocking temperature—leading to sharp inflection points in the Zijderveld plots between the ChRM and a secondary TRM/VRM. In MD grains, however, different grains will have different unblocking temperatures even for the same thermomagnetic history: The unblocking temperature depends on the combination of H_K, V, and V_{Bark} of the MD grain, in addition to the thermomagnetic history (i.e., acquisition time and temperature). Hence, in a natural sample that contains an assemblage of many different MD grains, some of these will unblock at lower temperatures and some at higher temperatures: This gives rise to the curvature in the thermal demagnetization Zijderveld diagram (Figure 6a) that spreads over $\sim$ 100°C in our simulation (note, however, that the slight curvature in Figure 4 is not due to this effect, since all the grains in that simulation were identical up to the different H_K—the slight curvature is due to viscous relaxation on the experimental timescale that also occurs in SD assemblages). This is consistent with experimental observations in MD grains (Dunlop et al., 1997). Second, the same effect is even stronger in AF vector demagnetization plots (Figure 6b): Since the TRM/VRM acquisition depends on H_K, V and V_{Bark}, but the AF demagnetization is only dependent on H_K, there is no simple relationship between remanence acquisition time/temperature and AF demagnetizing field. In this case, the same is true for SD grains, because remanence acquisition is controlled by the product of V and H_K for SD grains, while AF demagnetization is only dependent on H_K. Despite these differences, MD grains are remarkably reliable to reconstruct paleomagnetic directions from vector

demagnetization diagrams. Comparing Figures 4 and 5 also confirms what has long been part of "common sense" knowledge in the paleomagnetic community: that MD grains that cause long pTRM tails/curvatures in thermal demagnetization plots can be easily removed using AF pretreatment with a few millitesla. For studies whose goal is the isolation of a ChRM carried by SD grains, AF pretreatment is hence an effective tool to demagnetize (weakly pinned) MD grains and obtain "pure" SD thermal demagnetization plots afterward.

4.3. Limitations of the Model

The theory presented here is an advancement over the single-DW jump-type MD theories by Néel (1955) and others in that it models the effect of repeated DW jumps. In order to obtain an analytical solution to the equations, a number of assumptions and approximations have been made, however, which limits the validity of the theory to certain cases.

First, like previous models, we assumed a two-domain/one-DW grain. This simplifies the model because no DW-DW interactions need to be considered. On the other hand, one might argue that DW-DW interactions may be negligible for grains not too far from equilibrium, in which case our model could be applied to multi-DW grains. The only difference in this case would be that the shape factor N depends on the number n of DWs: For a large number of walls it approaches the value of a SD cube, that is, $N = 1/3$, for a two-domain grain it is 0.127 (as used in this work). Hence, as a first-order approximation, one could use the above equations with different N values in function of the number of DWs. The main conclusions would, however, be identical to the ones made above.

Second, we approximated the hyperbolic functions in equations (20) and (21) by their first-order expansions. This was necessary to obtain a closed-form solution to the PDE; however, in principle, one can keep the hyperbolic functions and solve the PDE numerically. The first-order approximation assumes that the external field is small or, more precisely, that $NM - H$ is small. The approximation of a small field to approximate the hyperbolic tangent appearing in the Maxwell-Boltzmann distribution is also often made for SD grains—for MD grains the difference is that "a small field" is defined with respect to the current remanent magnetization of the grain (the NM-term), that is, the external field can be considered small if the corresponding equilibrium magnetization does not deviate too far from the present remanent magnetization. As the remanent magnetization generally should not deviate too much from the zero-remanence state, the difference is, however, largely technical, and we can safely assume that the equations hold for small external fields.

Third, when integrating the PDF (23) (which can be done by partial integration) we assumed that the probability of finding the DW at the boundaries of the grain is 0, that is, $p(x = x_{\text{left boundary}}) = p(x = x_{\text{right boundary}}) = 0$. While this seems intuitively correct, this approximation has some important implications: p can be shown to be a Maxwell-Boltzmann distribution (similar to SD grains, but with many states). Hence, also the states at the grain boundaries have a finite nonzero probability. The value of it depends on the width of the distribution—in general p has a narrow peak around the remanent magnetization, in which case the approximation holds. This narrow peak is due to the shape of the self-demagnetizing energy potential—that is, the parabolic term in equation (6), which makes the states at the grain boundaries energetically prohibitively expensive. However, the term has a temperature dependence through M_s^2, that is, it diminishes with increasing temperature. Moreover, assuming that H_K has the same temperature dependence as M_s, the temperature dependence of the self-demagnetizing term is equal to the temperature dependence of the pinning energy term. Hence, when increasing the temperature of a sample, the two terms diminish: While the reduced pinning fields makes it easier for DWs to jump, the reduced self-demagnetizing field is less effective at pushing the DWs toward the equilibrium position. The net effect is that the probability distribution spreads out: DWs are more likely to be found far from their equilibrium state at high temperatures. In this regime, the probability at the grain boundaries can become large—ultimately at very high temperatures (close to T_C) one would expect to obtain a constant probability distribution, that is, one where all PS are equally likely. This would ultimately demagnetize the grain (if all PS are equally likely, the net magnetization is 0). Due to the approximation made here, however, this effect is not taken care of, and even at temperatures near the Curie temperature, the equations would still predict a finite remanent magnetization and a finite relaxation time. In fact, equation (24) has a convex shape that approaches infinity at both very low and very high temperatures and has a finite minimum in between. This minimum value τ_{min} is easily found to occur at temperature T_{min}

$$\frac{T_{\text{min}}}{M_s(T_{\text{min}})} = \frac{\mu_0 V_{\text{Bark}} H_K}{k_B} \tag{30}$$

which yields a time of

$$\tau_{\min} = \frac{\tau_0 V H_{K0} \exp(1)}{4 N M_{s0} V_{\text{Bark}}}. \quad (31)$$

Hence, the theory is only valid for temperatures well below $T_{\min}$—above $T_{\min}$ the grain would start to get demagnetized though the spreading of the distribution of DW positions. Note that for some values of $(V, V_{\text{Bark}}, H_{K0})$, $\tau_{\min}$ may be larger than experimental timescales such that this theory cannot be used for such a grain.

It has to be pointed out that the latter limitation affects the applicability of the model to paleointensities: In paleointensity experiments (Coe, 1967; Thellier & Thellier, 1959), often a curvature is found in plot of pTRM gain versus NRM loss for MD-dominated samples (Paterson et al., 2015). This effect, known as pTRM tails, is different from the pTRM tails that manifest as a curvature in vector demagnetization plots (Dunlop et al., 1997): The latter is due to the inequality unblocking temperatures of different grains that experienced the same thermomagnetic history during NRM acquisition; paleointensity pTRM tails, however, are due to a different thermomagnetic behavior during the two repeated heatings in the laboratory (one in zero field and one in field; or one in negative field and one in positive field). Therefore, in order to explain paleointensity pTRM tails, a theory needs to be able to predict different behaviors for two repeated heatings during which all parameters (except the applied field) are held constant—the theory described here does not predict this (it only predicts different behaviors if the timescales between acquisition and demagnetization are vastly different, as is the case between NRM acquisition and thermal demagnetization experiment). This shortcoming may very well be due to (among others) the above mentioned approximation: For as the sample is heated to progressively higher temperatures in the paleointensity experiment, at some point the demagnetizing field will become weak enough to allow grains to demagnetize not by moving DWs toward the center position in the grain but by equally distributing DWs throughout any possible PS, including those close to the grain boundaries (a state that has zero net magnetization). Hence, at high temperatures grains should experience a stronger demagnetizing effect than predicted by the model, and this even in an applied field. On the flip side, however, these grains would also experience a stronger magnetizing effect on cooling in field, since some of the DWs would already be close to the equilibrium location anyway. Hence, the theory described here is one of thermoviscous, not pure thermal, remanence and does not describe high temperature effects in paleointensity experiments.

5. Conclusions

The theory presented here is an advancement over previous MD theories in that it considers the effect of repeated DW jumps over many PS. It has been shown that repeated jumps lead to time-temperature relationship of blocking that deviates from SD theory and from Néel-type MD theories (which made the same thermoviscous predictions as Néel SD theory). The time-temperature relationship is similar to its SD equivalent (i.e., Pullaiah nomograms) for MD grains that have strong pinning fields, or small grain sizes (e.g., 1 μm), but the devation is stronger for weakly pinned large MD grains. It is shown that while these grains are more viscous and have lower coercivities than their SD counterparts, they can nevertheless reliably record TRMs and VRMs and in many cases preserve them over geological timescales. The thermoviscous stability of MD grains was found to depend on three MD grain characteristics: the pinning coercivity H_K, the grain size V, and the Barkhausen volume V_{Bark}, rather than just two (H_K and V) as in the SD case. The nomograms for these grains can be used to predict the thermoviscous stability of MD grains, but due to the mixture of many different MD grains that are expected to occur in natural samples, vector demagnetization plots are likely to show some level of curvature due to the different blocking temperatures or different AF demagnetizing fields of different MD grains. Nevertheless, the curvature is found to be of sufficiently limited extent that accurate reconstruction of paleomagnetic directions should also be possible from MD-dominated samples.

Acknowledgments
T. A. B. is supported by a Boya Postdoctoral fellowship funded by Peking University. We are grateful for many helpful discussions with Greig Paterson. We also thank David Dunlop for constructive comments that helped improve the manuscript and Aleksey Smirnov for his editorial handling. The source code for the numerical calculation of the figures shown in this work are freely available on https://github.com/thomasberndt.

References

Almeida, T. P., Muxworthy, A. R., Kovács, A., Williams, W., Brown, P. D., & Dunin-Borkowski, R. E. (2016). Direct visualization of the thermomagnetic behaviour of pseudo-single-domain magnetite particles. *Science Advances*, *2*(April), 1–6.

Berndt, T. A., & Muxworthy, A. R. (2017). Dating Icelandic glacial floods using a new viscous remanent magnetization protocol. *Geology*, *45*(4), 339–342. https://doi.org/10.1130/G38600.1

Berndt, T. A., Ramalho, R. S., Valdez-Grijalva, M. A., & Muxworthy, A. R. (2017). Paleomagnetic field reconstruction from mixtures of titanomagnetites. *Earth and Planetary Science Letters*, *465*, 70–81. https://doi.org/10.1016/j.epsl.2017.02.033

Bertotti, G., Basso, V., & Magni, A. (1999). Stochastic dynamics in quenched-in disorder and hysteresis. *Journal of Applied Physics*, *85*(8), 4355–4357. https://doi.org/10.1063/1.369782

Biggin, A. J. (2006). First-order symmetry of weak-field partial thermoremanence in multi-domin (MD) ferromagnetic grains: 2. Implications for Thellier-Type paleointensity determination. *Earth and Planetary Science Letters*, *245*, 454–470. https://doi.org/10.1016/j.epsl.2006.02.034

Biggin, A. J., & Poidras, T. (2006). First-order symmetry of weak-field partial thermoremanence in multi-domain ferromagnetic grains. 1. Experimental evidence and physical implications. *Earth and Planetary Science Letters*, *245*(1-2), 438–453. https://doi.org/10.1016/j.epsl.2006.02.035

Church, N. S., Feinberg, J. M., & Harrison, R. J. (2011). Low-temperature domain wall pinning in titanomagnetite: Quantitative modeling of multidomain first-order reversal curve diagrams and AC susceptibility. *Geochemistry, Geophysics, Geosystems*, *12*, Q07Z27. https://doi.org/10.1029/2011GC003538

Cizeau, P., Zapperi, S., Durin, G., & Stanley, E. H. (1997). Dynamics of a ferromagnetic domain wall and the Barkhausen effect. *Physical Review Letters*, *79*(23), 4669–4672. https://doi.org/10.1103/PhysRevLett.79.4669

Coe, R. S. (1967). The determination of paleo-intensities of the Earth's magnetic field with emphasis on mechanisms which could cause non-ideal behavior in Thellier's method. *Journal of geomagnetism and geoelectricity*, *19*(3), 157–179. https://doi.org/10.5636/jgg.19.157

Conbhuí, P. Ó., Williams, W., Fabian, K., Ridley, P., Nagy, L., & Muxworthy, A. R. (2018). MERRILL: Micromagnetic Earth Related Robust Interpreted Language Laboratory. *Geochemistry, Geophysics, Geosystems*, *19*, 1080–1106. https://doi.org/10.1002/2017GC007279

Day, R. (1977). TRM and its variation with grain size. *Journal of geomagnetism and geoelectricity*, *29*(4), 233–265. https://doi.org/10.5636/jgg.29.233

Dunlop, D. J. (1983). On the demagnetizing energy and demagnetizing factor of a multidomain ferromagnetic cube. *Geophysical Research Letters*, *3*, 79–82. https://doi.org/10.1029/GL010i001p00079

Dunlop, D. J., Özdemir, Ö., & Schmidt, W. (1997). Paleomagnetism and paleothermometry of the Sydney Basin 2. Origin of anomalously high unblocking temperatures. *Journal of Geophysical Research*, *102*, 27,285–27,295. https://doi.org/10.1029/97JB02478

Dunlop, D. J., & Özdemir, Ö. (1997). *Rock magnetism: Fundamentals and frontiers* (595 pp.). Cambridge: Cambridge University Press. https://doi.org/10.1017/CBO9781107415324.004

Dunlop, D. J., & Xu, S. (1994). Theory of partial thermoremanent magnetization in multidomain grains. 1. Repeated identical barriers to wall motion (single microcoercivity). *Journal of Geophysical Research*, *99*(B5), 9005–9023. https://doi.org/10.1029/93JB02566

Everitt, C. W. F. (1962). Thermoremanent magnetization III. Theory of multidomain grains. *Philosophical Magazine*, *7*(76), 599–616. https://doi.org/10.1080/14786436208212627

Fabian, K. (2000). Acquisition of thermoremanent magentization in weak magnetic fields. *Geophysical Journal International*, *142*, 478–486.

Fabian, K. (2001). A theoretical treatment of paleointensity determination experiments on rocks containing pseudo-single or multi domain magnetic particles. *Earth and Planetary Science Letters*, *188*(1-2), 45–58. https://doi.org/10.1016/S0012-821X(01)00313-2

Fabian, K. (2003). Statistical theory of weak field thermoremanent magnetization in multidomain particle ensembles. *Geophysical Journal International*, *155*(2), 479–488. https://doi.org/10.1046/j.1365-246x.2003.02057.x

Fabian, K., Kirchner, A., Williams, W., Heider, F., Leibl, T., & Huber, A. (1996). Three-dimensional micromagnetic calculations for magnetite using FFT. *Geophysical Journal International*, *124*(1), 89–104. https://doi.org/10.1111/j.1365-246x.1996.tb06354.x

Fabian, K., & Shcherbakov, V. P. (2004). Domain state stabilization by iterated thermal magnetization processes. *Geophysical Journal International*, *159*(2), 486–494. https://doi.org/10.1111/j.1365-246x.2004.02394.x

Fu, R. R., Weiss, B. P., Lima, E. A., Harrison, R. J., Bai, X.-N., Desch, S. J., et al. (2014). Solar nebula magnetic fields recorded in the Semarkona meteorite. *Science*, *11*, 1–9. https://doi.org/10.1126/science.1258022

Gaunt, P. (1977). The frequency constant for thermal activitation of a ferromagnetic domain wall. *Journal of Applied Physics*, *48*(8), 3470–3474. https://doi.org/10.1063/1.324195

Kitaba, I., Hyodo, M., Katoh, S., Dettman, D. L., & Sato, H. (2013). Midlatitude cooling caused by geomagnetic field minimum during polarity reversal. *Proceedings of the National Academy of Sciences*, *110*(4), 1215–1220. https://doi.org/10.1073/pnas.1213389110

McClelland-Brown, E., & Sugiura, N. (1987). A kinematic model of TRM acquisition in multidomain magnetite. *Physics of the Earth and Planetary Interiors*, *46*(1-3), 9–23.

Muxworthy, A. R., Dunlop, D. J., & Williams, W. (2003). High-temperature magnetic stability of small magnetite particles. *Journal of Geophysical Research*, *108*(B5), 2281. https://doi.org/10.1029/2002JB002195

Muxworthy, A. R., & Williams, W. (1999). Micromagnetic calculation of hysteresis as a function of temperature in pseudo-single domain magnetite. *Geophysical Research Letters*, *26*(8), 1065. https://doi.org/10.1029/1999GL900176

Muxworthy, A. R., Williams, J., & Heslop, D. (2015). Testing the use of viscous remanent magnetisation to date flood events. *Frontiers in Earth Science*, *3*, 1–9. https://doi.org/10.3389/feart.2015.00001

Nagy, L., Williams, W., Muxworthy, A. R., Fabian, K., Almeida, T. P., Conbhuí, P. Ó., & Shcherbakov, V. P. (2017). Stability of equidimensional pseudo-single-domain magnetite over billion-year timescales. *Proceedings of the National Academy of Sciences*, *114*, 10356–10360. https://doi.org/10.1073/pnas.1708344114

Néel, L. (1944). Effet des cavites et des inclusions sur le champ coercitif. *Cah. Phys*, *25*, 21–44.

Néel, L. (1949). Théorie du traînage magnétique des ferromagnétiques en grains fins avec applications aux terres cuites. *Annales de Géophysique*. https://doi.org/10.1016/S0009-2509(00)00427-9

Néel, L. (1955). Some theoretical aspects of rock-magnetism. *Advances in Physics*, *4*(14), 191–243. https://doi.org/10.1080/00018735500101204

Paterson, G. A., Biggin, A. J., Hodgson, E., & Hill, M. J. (2015). Thellier-type paleointensity data from multidomain specimens. *Physics of the Earth and Planetary Interiors*, *245*, 117–133. https://doi.org/10.1016/j.pepi.2015.06.003

Pike, C. R., Roberts, A. P., Dekkers, M. J., & Verosub, K. L. (2001). An investigation of multi-domain hysteresis mechanisms using FORC diagrams. *Physics of the Earth and Planetary Interiors*, *126*(1-2), 11–25. https://doi.org/10.1016/S0031-9201(01)00241-2

Pullaiah, G., Irving, E., Buchan, K. L., & Dunlop, D. J. (1975). Magnetization changes caused by burial and uplift. *Earth and Planetary Science Letters*, *28*, 133–143. https://doi.org/10.1016/0012-821X(75)90221-6

Sato, T., Nakamura, N., Goto, K., Kumagai, Y., Nagahama, H., & Minoura, K. (2014). Paleomagnetism reveals the emplacement age of tsunamigenic coral boulders on Ishigaki Island, Japan. *Geology*, *42*(7), 603–606. https://doi.org/10.1130/G35366.1

Schmidt, V. A. (1973). A multidomain model of thermoremanence. *Earth and Planetary Science Letters*, *20*(3), 440–446. https://doi.org/10.1016/0012-821X(73)90022-8

Shah, J., Williams, W., Almeida, T. P., Nagy, L., Muxworthy, A. R., Kovács, A., et al. (2018). The oldest magnetic record in our solar system identified using nanometric imaging and numerical modeling. *Nature Communications*, *9*(1173). https://doi.org/10.1038/s41467-018-03613-1

Shcherbakov, V. P., McClelland, E., & Shcherbakova, V. V. (1993). A model of multidomain thermoremanent magnetization incorporating temperature-variable domain structure. *Journal of Geophysical Research*, *98*(B4), 6201. https://doi.org/10.1029/92JB02572

Tarduno, J. A., Blackman, E. G., & Mamajek, E. E. (2014). Detecting the oldest geodynamo and attendant shielding from the solar wind: Implications for habitability. *Physics of the Earth and Planetary Interiors*, *233*, 68–87. https://doi.org/10.1016/j.pepi.2014.05.007

Thellier, E., & Thellier, O. (1959). Sur l'intensité du champ magnétique terrestre dans le passe historique et géologique. *Annales de Géophysique*, *15*, 285–376.

Valdez-Grijalva, M. A., Nagy, L., Muxworthy, A. R., Williams, W., & Fabian, K. (2018). The magnetic structure and palaeomagnetic recording fidelity of sub-micron greigite (Fe3S4). *Earth and Planetary Science Letters*, *483*, 76–89. https://doi.org/10.1016/j.epsl.2017.12.015

Valet, J. P., & Valladas, H. (2010). The Laschamp-Mono lake geomagnetic events and the extinction of Neanderthal: A causal link or a coincidence? *Quaternary Science Reviews*, *29*(27-28), 3887–3893. https://doi.org/10.1016/j.quascirev.2010.09.010

Xu, S., & Dunlop, D. J. (1994). Theory of partial thermoremanent magnetization in multidomain grains. 2. Effect of microcoercivity distribution and comparison with experiment. https://doi.org/10.1029/93JB02571

Zijderveld, J. D. A. (1967). AC demagnetization of rocks: Analysis of results. In D. Collinson, K. Creer, & S. Runcorn (Eds.), *Methods in paleomagnetism* (pp. 254–286). Amsterdam: Elsevier.